Nonlinear vibration analysis of a rotor system with parallel and angular misalignments under uncertainty via a Legendre collocation approach

Chao Fu[1,2†], Yongfeng Yang[1], Kuan Lu[1], Fengshou Gu[2]

[1]Institute of Vibration Engineering, Northwestern Polytechnical University, Xi'an 710072, China
[2]Centre for Efficiency and Performance Engineering, University of Huddersfield, Queensgate, Huddersfield, HD1 3DH, United Kingdom
[†]Corresponding author: fuchao0606@mail.nwpu.edu.cn; fuchaouk@gmail.com

Abstract

In this paper, the propagation of bounded uncertainties in the dynamic response of a misaligned rotor is investigated using a Legendre collocation based non-intrusive analysis method. A finite element rotor model is used and the parallel and angular misalignments are modelled by additions of stiffness and force terms to the system. A simplex meta-model for the harmonic solutions of the vibration problem is constructed to take into account the uncertainties. The influences of uncertainties in the fault parameters are analysed and the calculation performance of the interval method is validated. Different propagation mechanisms of the uncertainties are observed in the interval responses and discussed in case studies. The results of this study will promote the understandings of the nonlinear vibrations in misaligned rotor systems with interval variables.

Keywords: rotor; misalignment; bounded uncertainty; harmonic response; Legendre collocation

1. Introduction

Rotating machineries have wide applications in industrial fields and play an important role in both the civil economics and military services (Roy and Meguid 2018; Biswas and Ray 2013; Lu et al. 2018). Typical faults such as a crack may occur during operation, which will cause harmful vibrations (Ma et al. 2015a). The stability of rotor systems mounted on journal bearings with multi slip zones was studied by Bhattacharya et al. (2017). Li et al. (2019) investigated the nonlinear dynamics of a rotor supported by nonlinear supports at both ends and the effect of rubbing was analysed. Residual bow was found to have a significant effect on the first order critical speed of the geared system with stiff viscoelastic supports (Kang et al. 2011). Misalignment is deemed to be the second most common fault after out of balance and they often exist simultaneously (Patel and Darpe 2009; Wang and Jiang 2018; Srinivas et al. 2019). Assembling error, long time operation and thermal effects are contributories to these faults. Extra reacting forces and moments will be generated and the dynamics including stability of the rotor system can be significantly influenced (Ma et al. 2015b; Tuckmantel and Cavalca 2019; Al-Hussain 2003). In rotor systems, there are generally two types of misalignment, i.e. the parallel misalignment and the angular misalignment. The modelling methods and various dynamic behaviors in misaligned rotors have been investigated by many researchers worldwide. Li et al. (2012) established the

mathmatical model of a rotor system in aero-engine subject to misalignment and unbalance coupling faults. Wang et al. (2015) used an additional stiffness term to simulate the effect of angular misalignment and derived the motion equations of a four-degrees-of-freedom rotor system. Li et al. (2016; 2017) modelled angular misalignment based on the geometric constraints between the adjacent coordinates. Lees (2007) proposed the modelling method for parallel misalignment using the Lagrange's formulation where shafts are connected by a number of bolts. The technique was further used to analyse angular misalignment (Didier et al. 2012a). Sinha et al. (2004) proposed an estimation method for the misalignment and unbalance faults based on only one run-down process. Its robustness was verified via sensitivity analysis on rotor bearing models. Xu and Marangoni (1994) carried out the experimental validation for dynamic characteristics of an unbalanced rotor system with misalignment and revealed some in-depth vibration behaviours at the $2\times$ rotating speed of the system.

In the design stage, it is very hard to accurately simulate the actual operational conditions and physical parameters will have critical impacts on the vibration characteristics of rotor systems. Errors and extra variations may be introduced in manufacturing, service and maintenance periods (Liu et al. 2016; Jiang et al. 2012). In other words, there are ubiquitous uncertainties in the physical models, excitations and classic faults. The corresponding dynamic behaviours can deviate from the design values and further cause instabilities or severe failures (Fu et al. 2017). This is especially true for misaligned rotors, which may be affected by manual assemble errors or small defects in couplings. In engineering, it often happens that the vibration will deteriorate when a well-balanced rotor is reassembled. The uncertainty analysis for rotordynamics has attracted attention in recent years. Some studies have been reported in the literature (Yang et al. 2019; Lu et al. 2019; Sinou et al. 2018; Fu et al. 2018a, 2018b; Didier et al 2012b; Koroishi et al. 2012; Ritto et al. 2011; Sinou and Faverjon 2012), which were devoted to investigating the linear and nonlinear dynamics of rotor systems under various uncertain conditions based on both the stochastic and non-probabilistic approaches. More specifically, Li et al. (2016; 2017) studied the random nonlinear vibration characteristics of a rotor system with angular misalignment and nonlinear bearings using the Polynomial Chaos Expansion (PCE). Multiple typical faults in a rotor system, including the parallel and angular misalignments, were considered by Didier et al. (2012a) and the influences of the stochastic fault parameters were investigated using the PCE. Li et al. (2012) and Wang et al. (2015) employed the Taylor interval method to reveal the uncertain dynamics of misaligned dual rotors simplified from the aero-engine. Some important factors should be considered in the uncertainty propagation analysis of misaligned rotor systems, i.e. the application prerequisites and implementation convenience of the propagation methods, the accuracy of the physical model and the underlying computational efficiency. The distribution model of uncertainty should be established in the probability-based methods or hypothesis should be made, which could be subjective. The Taylor interval analysis method is derivative-based and intrusive, which is only suitable for small range

uncertainty and is difficult to adapt to large-scale models or high-order problems. Therefore, they can only be used in systems with a few degrees of freedom. This paper will focus on the uncertainty propagation analysis of a finite element rotor model with both the parallel and angular misalignments. A Legendre collocation based non-intrusive interval surrogate is proposed for this purpose, which avoids complicated approximation theory and derivation operations in the previous methods. Large variations in the uncertainties can be applied. Efforts aimed at reducing the computation burden are incorporated to deal with multi-dimensional uncertainties. The high efficiency and accuracy, as well as the uncomplicated implementation of the method will be demonstrated via case studies. The variability patterns of the responses due to the uncertainties in the two types of misalignment will be revealed.

The remainder of the content is as follows. The modelling process of the parallel and angular misalignments will be briefly explained in Section 2. Section 3 presents the steps and principles of the uncertainty propagation method. Numerical simulation with uncertainties in the fault parameters will be given in Section 4. Some conclusions are summarised in the last section.

2. Misalignment modelling and the deterministic motion equation

The finite element method (FEM) has been widely used to model the rotating systems and establish the governing equations of motion in relation to the lateral vibration (Friswell et al. 2010). For a general rotor-disk-bearing system, the modelling of the Euler beam elements, mass disks and linear isotropic bearing elements is standard. The matrices for different typical elements and the assemblage technique will not be described in the current study and the readers are referred to Friswell et al. (2010) for further instructions. Generally, the governing motion equation of a rotor-disk-bearing system can be represented as

$$\mathbf{M}\ddot{\mathbf{q}}(t)+(\mathbf{C}+\omega\mathbf{G})\dot{\mathbf{q}}(t)+\mathbf{K}\mathbf{q}(t)=\mathbf{F}(t) \tag{1}$$

where $\mathbf{M}$, $\mathbf{C}$, $\mathbf{K}$ and $\mathbf{G}$ are, respectively, the global mass, damping, stiffness and gyroscopic matrices of the system. The acceleration, velocity and displacement vectors are denoted by $\ddot{\mathbf{q}}(t)$, $\dot{\mathbf{q}}(t)$ and $\mathbf{q}(t)$, respectively. $\mathbf{F}(t)$ is the unbalance and gravitational forces. ω represents the angular speed of the shaft. All quantities given in Eq. (1) are formulated in the fixed coordinate system.

2.1. Parallel misalignment

In this subsection, the effects of the parallel misalignment on the system will be modelled. The two rotors connected by coupling with *N* bolted joints are assumed to be operating at a synchronized rotating speed. The bolts are distributed on a circle at a radius r_p from the shaft centerline and they have a transverse stiffness k_t. Suppose the centerlines of the two shafts have a relative vertical displacement δ_p, the schematic configuration of the fault is illustrated in Fig. 1. Obviously, the effects are exaggerated here to show the relationship although the displacement is generally small in reality.

As the bolts are evenly distributed in a circumference, their angles can be defined as

$$\alpha_i = \frac{i-1}{N}\pi, \quad i = 1,\ 2,\ \cdots,\ N \tag{2}$$

According to the geometrical relationship, the position of the *i*th bolt on the two rotors in fixed coordinate frame can be given as (Lees 2007; Didier et al. 2012a)

$$\boldsymbol{OM}_1^i = \begin{bmatrix} v \\ w \\ 0 \end{bmatrix} + \begin{bmatrix} -r\sin(\omega t + \alpha_i) \\ r\cos(\omega t + \alpha_i) \\ r\varphi\cos(\omega t + \alpha_i) + r\beta\sin(\omega t + \alpha_i) \end{bmatrix} \tag{3}$$

$$\boldsymbol{OM}_2^i = \begin{bmatrix} -r\sin(\omega t + \alpha_i) - \delta_p\sin(\omega t) \\ r\sin(\omega t + \alpha_i) - \delta_p(1-\cos(\omega t)) \\ 0 \end{bmatrix} \tag{4}$$

where $[v\ w\ \varphi\ \beta]^T$ denotes the nodal lateral displacement vector of the coupling and t is time. Then the sum of strain energy of bolts can be given as

$$E_{pm} = \frac{1}{2}Nk_t[(v + \delta_p\sin(\omega t))^2 + (w + \delta_p(1-\cos(\omega t)))^2] \tag{5}$$

After the Lagrange's operation, the effects of parallel misalignment will be represented by an additional stiffness term and a force term on the coupling node (Didier et al. 2012a; El-Mongy and Younes 2018)

$$\mathbf{K}_{pm} = Nk_t diag(1,\ 1,\ 0,\ 0) \tag{6}$$

$$\mathbf{F}_{pm} = Nk_b\delta_p[\sin(\omega t),\ 1-\cos(\omega t),\ 0,\ 0]^T \tag{7}$$

2.2. Angular misalignment

The angular misalignment can be modelled similarly to the previous method. The bolts will have an axial stiffness k_a and the first one will have the stiffness $k_a + k'$ in z direction (Didier et al. 2012a). Suppose the magnitude of angular misalignment is δ_a, a schematic diagram showing the configuration of the fault is presented in Fig. 2. Similarly, the magnitude of the angular misalignment is small and it is intentionally magnified.

The positions of bolts are calculated in the fixed frame as

$$\boldsymbol{O}_2\boldsymbol{M}_2^i = \begin{bmatrix} -r\sin(\omega t + \alpha_i) \\ r\cos(\omega t + \alpha_i) \\ r\delta_a\cos(\omega t + \alpha_i) \end{bmatrix} \tag{8}$$

Then the strain energy of bolts can be given as

$$E_{am} = \sum_i^N \frac{1}{2}r^2k_i[(\varphi - \delta_a)\cos(\omega t + \alpha_i) + (\beta\cos(\omega t + \alpha_i)]^2 \tag{9}$$

By Lagrange's calculation, one can describe the effects of angular misalignment using a time-variant stiffness term and a two-order harmonic force term (Didier et al. 2012a)

$$\mathbf{K}_{am} = \frac{1}{2}(3k_a + k')r^2 \begin{bmatrix} 0 & & & \\ & 0 & & \\ & & 1 & \\ & & & 1 \end{bmatrix} + \frac{1}{2}k'r^2 \begin{bmatrix} 0 & & & \\ & 0 & & \\ & & \cos(2\omega t) & \sin(2\omega t) \\ & & \sin(2\omega t) & -\cos(2\omega t) \end{bmatrix} \tag{10}$$

$$\mathbf{F}_{pm} = -\frac{1}{2}r^2\delta_p[0,\ 0,\ 3k_a + k'(1+\cos(2\omega t)),\ k'\sin(2\omega t)]^T \tag{11}$$

Considering the effects of the parallel and angular misalignments on the rotor, the motion equations of the misaligned system can be written as

$$\begin{aligned} \mathbf{M}\ddot{\mathbf{q}} + (\mathbf{C} + \omega\mathbf{G})\dot{\mathbf{q}} + (\mathbf{K}_0 + \mathbf{K}_c\cos(2\omega t) + \mathbf{K}_s\sin(2\omega t))\mathbf{q} = \\ \mathbf{F}_0 + \mathbf{F}_{c1}\cos(\omega t) + \mathbf{F}_{s1}\sin(\omega t) + \mathbf{F}_{c2}\cos(2\omega t) + \mathbf{F}_{s2}\sin(2\omega t) \end{aligned} \tag{12}$$

where $\mathbf{K}_0$ is a constant stiffness matrix, including $\mathbf{K}$ in Eq. (1), the stiffness in Eq. (6) and the constant part in Eq. (10). $\mathbf{K}_c$ and $\mathbf{K}_s$ are the stiffness matrices of the second order harmonics. $\mathbf{F}_0$ is the constant part of the forces on the system. $\mathbf{F}_{c1}$ and $\mathbf{F}_{s1}$ are the force amplitudes of the first order harmonics whilst $\mathbf{F}_{c2}$ and $\mathbf{F}_{s2}$ are those of the second order harmonics.

Given the form of Eq. (12), the harmonic balance method (HBM) (Nayfeh and Mook 2008), a fast method for steady-state solutions, can be conveniently employed to solve the dynamic response of the system. The forces on the system shown in the right hand side of Eq. (12) are already in harmonic form. The displacement vector can then be expressed in finite Fourier expansion

$$\mathbf{q}(t) = \mathbf{A}_0 + \sum_{k=1}^{n}\left(\mathbf{A}_k\cos(k\omega t) + \mathbf{B}_k\sin(k\omega t)\right) \tag{13}$$

where n is the truncation order. Order 4 will be adequate for the present study according to previous nonlinear analyses of faulty rotor systems (Sinou and Faverjon 2012; Tai et al. 2015; Yang et al. 2019). Then magnitude of the *j*-th order harmonic component of the dynamic response can be calculated as

$$\sqrt{\mathbf{A}_k^2 + \mathbf{B}_k^2},\ k = 0,\ 1,\ \cdots,\ n \tag{14}$$

Submit Eq. (13) into Eq. (12) and balance the coefficients of the same order harmonic terms, it will generate a set of linear equations

$$\mathbf{H}\mathbf{X} = \mathbf{\Gamma} \tag{15}$$

where

$$\mathbf{X} = [\mathbf{A}_0,\ \mathbf{A}_1,\ \mathbf{B}_1,\ \cdots,\ \mathbf{A}_n,\ \mathbf{B}_n]^T \tag{16}$$

$$\mathbf{\Gamma} = [\mathbf{F}_0,\ \mathbf{F}_{c1},\ \mathbf{F}_{s1},\ \mathbf{F}_{c2},\ \mathbf{F}_{s2},\ \mathbf{0},\ \cdots,\ \mathbf{0}]^T \tag{17}$$

154 $$\mathbf{H}=\begin{bmatrix}
\mathbf{K}_0 & \mathbf{0} & \mathbf{0} & 0.5\mathbf{K}_1 & 0.5\mathbf{K}_2 & \mathbf{0} & \mathbf{0} & \mathbf{0} & \mathbf{0} & \cdots & \mathbf{0} & \mathbf{0} \\
\mathbf{0} & \mathbf{\Lambda}^{(1)}+0.5\mathbf{K}_1 & \tilde{\mathbf{\Lambda}}^{(1)}+0.5\mathbf{K}_2 & \mathbf{0} & \mathbf{0} & 0.5\mathbf{K}_1 & 0.5\mathbf{K}_2 & \mathbf{0} & \mathbf{0} & \cdots & \mathbf{0} & \mathbf{0} \\
\mathbf{0} & -\tilde{\mathbf{\Lambda}}^{(1)}+0.5\mathbf{K}_2 & \mathbf{\Lambda}^{(1)}-0.5\mathbf{K}_1 & \mathbf{0} & \mathbf{0} & -0.5\mathbf{K}_2 & 0.5\mathbf{K}_1 & \mathbf{0} & \mathbf{0} & \cdots & \mathbf{0} & \mathbf{0} \\
2\mathbf{K}_1 & \mathbf{0} & \mathbf{0} & \mathbf{\Lambda}^{(2)} & \tilde{\mathbf{\Lambda}}^{(2)} & \mathbf{0} & \mathbf{0} & 0.5\mathbf{K}_1 & 0.5\mathbf{K}_2 & \ddots & \mathbf{0} & \mathbf{0} \\
2\mathbf{K}_2 & \mathbf{0} & \mathbf{0} & -\tilde{\mathbf{\Lambda}}^{(2)} & \mathbf{\Lambda}^{(2)} & \mathbf{0} & \mathbf{0} & -0.5\mathbf{K}_2 & 0.5\mathbf{K}_1 & \ddots & \vdots & \vdots \\
\mathbf{0} & 0.5\mathbf{K}_1 & 0.5\mathbf{K}_2 & \mathbf{0} & \mathbf{0} & \mathbf{\Lambda}^{(3)} & \tilde{\mathbf{\Lambda}}^{(3)} & \mathbf{0} & \mathbf{0} & \ddots & \mathbf{0} & \mathbf{0} \\
\mathbf{0} & -0.5\mathbf{K}_2 & 0.5\mathbf{K}_1 & \mathbf{0} & \mathbf{0} & -\tilde{\mathbf{\Lambda}}^{(3)} & \mathbf{\Lambda}^{(3)} & \mathbf{0} & \mathbf{0} & \ddots & 0.5\mathbf{K}_1 & 0.5\mathbf{K}_2 \\
\mathbf{0} & \mathbf{0} & \mathbf{0} & 0.5\mathbf{K}_1 & 0.5\mathbf{K}_2 & \mathbf{0} & \mathbf{0} & \mathbf{\Lambda}^{(4)} & \tilde{\mathbf{\Lambda}}^{(4)} & \ddots & -0.5\mathbf{K}_2 & 0.5\mathbf{K}_1 \\
\mathbf{0} & \mathbf{0} & \mathbf{0} & -0.5\mathbf{K}_2 & 0.5\mathbf{K}_1 & \mathbf{0} & \mathbf{0} & -\tilde{\mathbf{\Lambda}}^{(4)} & \mathbf{\Lambda}^{(4)} & \ddots & \mathbf{0} & \mathbf{0} \\
\vdots & \vdots & \vdots & \ddots & \ddots & \ddots & \ddots & \ddots & \ddots & \ddots & \mathbf{0} & \mathbf{0} \\
\mathbf{0} & \mathbf{0} & \mathbf{0} & \mathbf{0} & \cdots & \mathbf{0} & 0.5\mathbf{K}_1 & 0.5\mathbf{K}_2 & \mathbf{0} & \mathbf{0} & \mathbf{\Lambda}^{(n)} & -\tilde{\mathbf{\Lambda}}^{(n)} \\
\mathbf{0} & \mathbf{0} & \mathbf{0} & \mathbf{0} & \cdots & \mathbf{0} & -0.5\mathbf{K}_2 & 0.5\mathbf{K}_1 & \mathbf{0} & \mathbf{0} & -\tilde{\mathbf{\Lambda}}^{(n)} & \mathbf{\Lambda}^{(n)}
\end{bmatrix}$$

155 (18)

156 where $\mathbf{\Lambda}^{(s)}=\mathbf{K}_0-(s\omega)^2\mathbf{M}$ and $\tilde{\mathbf{\Lambda}}^{(s)}=s\omega(\mathbf{C}+\omega\mathbf{G})$, $s=1, 2, \ldots, n$. Then the unknown Fourier
157 coefficients, i.e. the steady-state dynamic responses, can be solved by Eq. (15).

158 ## 3. Legendre collocation approach for uncertainty quantification

159 In the above modelling, uncertainties in the fault parameters are not included. This section will establish
160 the propagation model of bounded uncertainties in the harmonic responses. As discussed previously,
161 the non-intrusive and non-probabilistic uncertainty propagation procedures will prevail in complicated
162 engineering systems with little prior statistic information. Some interval analysis methods and surrogate
163 modelling techniques (Qiu and Wang 2003; Wu et al. 2013, 2016; Elishakoff and Sarlin 2016; Soize
164 2001; Qi and Qiu 2012) have been proposed for dynamic analysis of the uncertain truss structures and
165 multibody systems. Here, a Legendre collocation scheme is proposed to establish a simple meta-model
166 for the uncertain harmonic solutions. Firstly, the uncertain-but-bounded magnitude of the parallel
167 misalignment is expressed in interval form

168 $$\delta_p^I=[\delta_p^c-\alpha_1\delta_p^c,\ \delta_p^c+\alpha_1\delta_p^c] \tag{19}$$

169 where superscripts *I* and *c* denote the interval quantity and its nominal value. α_1 is the uncertainty
170 range indicator for the parallel misalignment. Similarly, the uncertain magnitude of the angular
171 misalignment can also be written as

172 $$\delta_a^I=[\delta_a^c-\alpha_2\delta_a^c,\ \delta_a^c+\alpha_2\delta_a^c] \tag{20}$$

173 where α_2 is its uncertainty indicator. More indicators will be generated if other physical parameters
174 are to be considered uncertain and a standard uncertain variable vector $\boldsymbol{\alpha}=\{\alpha_1, \alpha_2, \alpha_3,\cdots\}$ can be
175 defined, which represents all the indicators. In the presence of interval parameters, the response output
176 of the rotor will also be uncertain. The harmonic solutions in Eq. (15) can be expressed as

177 $$\begin{cases}\mathbf{A}_i^I=[\underline{\mathbf{A}}_i, \overline{\mathbf{A}}_i], & i=0, 1, \ldots, n\\ \mathbf{B}_j^I=[\underline{\mathbf{B}}_j, \overline{\mathbf{B}}_j], & j=1, 2, \ldots, n\end{cases} \tag{21}$$

178 where an underscore represents the lower bound (LB) and an overbar denotes the upper bound (UB).
179 Solving the uncertain dynamic problem is equivalent to determining the bounds of the interval harmonic
180 solutions expressed in Eq. (21). The meta-modelling technique can be used for this purpose. In the

following, the interval modelling method for any harmonic solutions of interest will be explained. It could be either the Fourier coefficient of a single component or all of them in a row. Naturally, the uncertain solution will be a function of the vector $\boldsymbol{\alpha}$, which can be denoted as $f(\boldsymbol{\alpha})$.

To establish the surrogate function, the basics of the Legendre orthogonal series should be described. The recursive relationships of Legendre polynomials are as follows

$$\begin{cases} L_0(x)=1, \;\; L_1(x)=x; \\ (n+1)L_{n+1}(x)=(2n+1)xL_n(x)-nL_{n-1}(x) \end{cases} \tag{22}$$

They are orthogonal on standard interval [-1, 1] with a constant weight function $\rho(x)\equiv 1$. The zeros of the Legendre polynomial $\boldsymbol{\xi}=\{\xi_i\}$, which are already defined according to the polynomial expression, can be used as samples in the uncertain parameter space due to their distribution structure. It is worth mentioning that approximation of the uncertain response via the Gauss-Legendre quadrature will not be adopted due to the complexity in deduction. Instead, a regression form involving less mathematic efforts will be outlined. Suppose there are *m* uncertain parameters, we can predefine a *p*-order regression model for the uncertain response in a way similar to the response surface method

$$f(\boldsymbol{\alpha})=\sum_{k=0}^{p}\boldsymbol{\varphi}^{(k)}\mathbf{S}^{(k)}(\boldsymbol{\alpha}) \tag{23}$$

where $\boldsymbol{\varphi}^{(k)}$ is the unknown coefficient vector with the same size of $\mathbf{S}^{(k)}$. $\mathbf{S}^{(k)}$ is the vector for all the combinations of terms $\alpha_1^{i_1}\alpha_1^{i_2}\cdots\alpha_m^{i_m}$ satisfying

$$\sum_{j=1}^{m} i_j = i_1+i_2+\cdots+i_m = k \tag{24}$$

We have $\mathbf{S}^{(0)}=[1]$ and

$$\begin{cases} \mathbf{S}^{(1)}=[\alpha_1,\ \alpha_2,\ \cdots,\ \alpha_{m-1},\ \alpha_m]^T \\ \mathbf{S}^{(2)}=[\alpha_1^2,\ \alpha_1\alpha_2,\ \alpha_1\alpha_3,\cdots,\ \alpha_m^2]^T \\ \quad\vdots \\ \mathbf{S}^{(p)}=[\alpha_1^p,\ \alpha_1^{p-1}\alpha_2,\ \alpha_1^{p-1}\alpha_3,\ \cdots,\ \alpha_m^p]^T \end{cases} \tag{25}$$

In Eq. (23), the coefficient vector $\boldsymbol{\varphi}=[\boldsymbol{\varphi}^{(1)},\ \boldsymbol{\varphi}^{(2)},\ \cdots,\ \boldsymbol{\varphi}^{(p)}]$ should be determined to fully construct the model. The dimension of vector $\boldsymbol{\varphi}$ is $\tilde{n}=(m+p)!/m!/p!$. Let $\mathbf{S}=[1,\ \mathbf{S}^{(1)},\ \mathbf{S}^{(2)},\ \cdots,\ \mathbf{S}^{(p)}]^T$, it further leads to the following expression

$$f(\boldsymbol{\alpha})=\boldsymbol{\varphi}\mathbf{S}(\boldsymbol{\alpha}) \tag{26}$$

For each uncertainty indicator α_i, the least number of collocations should be $n'=p+1$. These collocations can be generated by the zeros of the n'-order Legendre polynomial. In problems with single uncertainty, all the collocations should be used to estimate the unknown coefficients. When multiple uncertainties are taken into consideration, strategies aimed to reduce the computational efforts should be introduced. It was proposed that $2\tilde{n}$ collocations, i.e. two times of the dimension of $\boldsymbol{\varphi}$, will give robust results and achieve good efficiency (Isukapalli 1999; Wu et al. 2015). The collocations will be drawn randomly from the tensorial candidate space

$$\hat{\boldsymbol{\xi}}_{2n\times m}\subset\left\{\boldsymbol{\xi}_{1,n'\times 1}\otimes\boldsymbol{\xi}_{2,n'\times 1}\otimes\cdots\otimes\boldsymbol{\xi}_{m,n'\times 1}\right\} \tag{27}$$

At each collocation set $\hat{\boldsymbol{\xi}}(j,\ 1{:}\ m)$, the deterministic harmonic solution can be evaluated by Eq. (15) as

$$\hat{\mathbf{X}} = \{\hat{\mathbf{X}}_j,\ j = 1,\ 2,\ \cdots,\ 2\tilde{n}\} \tag{28}$$

$$\hat{\mathbf{X}}_j(\hat{\boldsymbol{\xi}}_j) = \mathbf{H}^{-1}(\hat{\boldsymbol{\xi}}_j)\boldsymbol{\Gamma}(\hat{\boldsymbol{\xi}}_j) \tag{29}$$

It should be noted that Eq. (29) represents a deterministic simulation as the uncertain parameters are all specified to fixed collocations. As a non-intrusive scheme, this is the only step where the rotor system model is involved and the deterministic modelling of the misalignment faults in Section 2 is integrated into the uncertainty propagation procedure. In other words, they are actually working independently and no further modifications to the established solver are needed in different uncertain cases. At the same time, the sample outputs of the $\mathbf{S}$ matrix should be calculated

$$\hat{\mathbf{S}} = \{\hat{\mathbf{S}}_j,\ j = 1,\ 2,\ \cdots,\ 2\tilde{n}\} \tag{30}$$

$$\hat{\mathbf{S}}_j(\hat{\boldsymbol{\xi}}_j) = [1,\ \mathbf{S}^{(1)}(\hat{\boldsymbol{\xi}}_j),\ \mathbf{S}^{(2)}(\hat{\boldsymbol{\xi}}_j),\ \cdots,\ \mathbf{S}^{(p)}(\hat{\boldsymbol{\xi}}_j)]^T \tag{31}$$

Then, the unknown coefficient vector $\boldsymbol{\varphi}$ can be estimated in regression form as

$$\boldsymbol{\varphi} = \hat{\mathbf{X}}\hat{\mathbf{S}}(\hat{\mathbf{S}}^{\mathrm{T}}\hat{\mathbf{S}})^{-1} \tag{32}$$

The simplex meta-function of Eq. (26) is completely determined as long as the unknown coefficient vector is obtained. Ranges of the uncertain harmonic solutions can be easily estimated by this simple and explicit mathematical expression with respect to the standard variable vector $\boldsymbol{\alpha}$. The calculation performance will be assessed in the numerical simulation section and verifications will be provided.

4. Numerical results with case studies

In this section, numerical simulations regarding different uncertain parameters are carried out to investigate their effects on the vibration behaviours of the misaligned rotor. Here, only the model of the second rotor is presented as the first is rigid. Figure 3 shows the academic model of the rotor, which consists two rigid discs and is supported by two bearings at the two ends. It is discretized into 14 Euler beam elements with the torsional vibration being neglected. The two discs are located at node 3 and 12. The values of the model parameters are given in Table 1. Mass imbalance is considered at disc 2 and the rest of the rotor system is assumed to be well-balanced. All the responses will be drawn at node 2. The deterministic parallel misalignment is 0.001 m and the angular misalignment is 0.001 rad.

Firstly, the uncertainty in parallel misalignment is investigated. The varying range is taken as 10% of its mid-value. The uncertain results of the first four harmonic components using the 3-order surrogate procedure are demonstrated in Fig. 4. As clearly indicated in Fig. 4, the uncertainty in the parallel misalignment affects mainly the first order harmonic component and a small variability is noticed in the $3\times$ component. In the $2\times$ and $4\times$ components, the upper and lower response bounds stay close to the deterministic lines and no obvious response ranges are noticed. The results can be explained by referring to Eq. (7), which shows that the parallel misalignment will add a first-order harmonic force to the rotor system. The trivial variability in the third component is introduced by the coupling of the

first order and the third order components, which can be observed when applying the HBM.

It is important to validate the accuracy of the obtained uncertainty propagation results. To this end, the scanning method is used to provide reference solutions using 100 equally spaced samples in the interval of uncertain parallel misalignment. To validate the accuracy, it will be difficult to identify the differences in the response bound curves between the reference solutions and those from the surrogate method since they are very close to each other. Instead, the difference rate diagram for the upper and lower bounds is provided by taking the reference solutions as accurate ones, as shown in Fig. 5. The magnitudes of difference rates in Fig. 5 for the UB and LB demonstrate that the two categories of results are almost identical for the $2\times$ and $4\times$ components. The largest rates appear in the $1\times$ and $3\times$ components, but they are actually small (less than 1%). The simulation tasks are carried out on a personal laptop operating Windows 10 with Intel Core i7-8550U@1.8GHz and 16GB RAM. The average CPU time for the proposed Legendre method is 69.55 s whilst for the scanning method it is 3766.72 s. The calculation efficiency is verified by this comparison. In fact, the deterministic model will be evaluated for every sample to gather all the sample harmonic responses. The advantage will be significant if the rotor model has many degrees of freedom. Thus, the effectiveness of the proposed method is validated.

Figure 6 presents the influence of 5% bounded uncertainty in the angular misalignment on the harmonic responses of the rotor system. An obvious phenomenon contrary to that in the case of uncertain parallel misalignment can be seen. In Fig. 6, variabilities of the responses only appear at the $2\times$ and $4\times$ components whilst no visible fluctuations are observed in the $1\times$ and $3\times$ components, which can be evidenced by Eqs. (10) and (11). The effects of angular misalignment are expressed in second order harmonic form and coupling effects will be introduced. Furthermore, the case with multi uncertainties in different physical parameters is considered. Using the same 3-order surrogate, Fig. 7 gives the variability of the vibration response of the rotor system under 5% uncertainties in both the misalignments, 10% uncertainty in the unbalance and 2% uncertainty in the stiffness of bearing 2. With those multiple uncertainties present, the traditional sampling-based scanning method will be computationally prohibitive due to the geometrical growing samples. However, the bounds of the harmonic components in Fig. 7 are smooth which shows the robustness of the surrogate. The variability of dynamic response also indicates that the propagation of uncertainties causes significant deviations in the deterministic harmonic solutions. As expected, all of the four harmonic components are affected by the multiple uncertain parameters.

5. Conclusions

A finite element rotor model with both parallel and angular misalignments is considered in this paper to investigate the propagation of non-probabilistic uncertainties in the dynamic responses. The HBM coupled with a non-intrusive Legendre collocation based surrogate method is used to obtain the ranges of the harmonic solutions. The uncertainty in parallel misalignment propagates only into the $1\times$ and

$3\times$ components whilst the uncertainty in angular misalignment affects the $2\times$ and $4\times$ components. Multi uncertainties will demonstrate significant influences on all of the harmonic components of the dynamic responses. Moreover, the effectiveness of the proposed method is validated via the scanning method. The method is also suitable for the uncertainty analysis of general engineering structures.

Acknowledgements

This work is financially supported by the National Natural Science Foundation of China (No. 11272257) and the Fundamental Research Funds for the Central Universities (No. 3102018ZY016).

References

Al-Hussain, K.M.: Dynamic stability of two rigid rotors connected by a flexible coupling with angular misalignment. J. Sound Vib. **266**(2), 217-234 (2003)

Biswas, D., Ray, M.C.: Active constrained layer damping of geometrically nonlinear vibration of rotating composite beams using 1-3 piezoelectric composite. Int. J. Mech. Mater. Des. **9**(1), 83-104 (2013)

Bhattacharya, A., Dutt, J.K., Pandey, R.K.: Influence of hydrodynamic journal bearings with multiple slip zones on rotordynamic behavior. J. Tribol. **139**(6), 061701 (2017)

Didier, J., Sinou, J.-J., Faverjon, B.: Study of the non-linear dynamic response of a rotor system with faults and uncertainties. J. Sound Vib. **331**(3), 671-703 (2012a)

Didier, J., Faverjon, B., Sinou, J.-J.: Analysing the dynamic response of a rotor system under uncertain parameters by polynomial chaos expansion. J. Vib. Control **18**(5), 712-732 (2012b)

El-Mongy, H.H, Younes, Y.K.: Vibration analysis of a multi-fault transient rotor passing through sub-critical resonances. J. Vib. Control **24**(14), 2986-3009 (2018)

Elishakoff, I., Sarlin, N.: Uncertainty quantification based on pillars of experiment, theory, and computation. Part II: Theory and computation. Mech. Syst. Signal Process **74**, 54-72 (2016)

Friswell, M.I., Penny, J.E., Lees, A.W., Garvey, S.D.: Dynamics of rotating machines. Cambridge University Press, 2010.

Fu, C., Ren, X., Yang, Y., Xia, Y., Deng, W.: An interval precise integration method for transient unbalance response analysis of rotor system with uncertainty. Mech. Syst. Signal Process **107**, 137-148 (2018a)

Fu, C., Ren, X., Yang, Y., Lu, K., Wang, Y.: Nonlinear response analysis of a rotor system with a transverse breathing crack under interval uncertainties. Int. J. Nonlin. Mech. **105**, 77-87 (2018b)

Fu, C., Ren, X., Yang, Y., Qin, W.: Dynamic response analysis of an overhung rotor with interval uncertainties. Nonlinear Dynam. **89**(3), 2115-2124 (2017)

Isukapalli, S.S.: Uncertainty analysis of transport-transformation models. The State University of New Jersey, New Brunswick (1999)

Jiang, C., Lu, G., Han, X., Liu, L.: A new reliability analysis method for uncertain structures with random and interval variables. Int. J. Mech. Mater. Des. **8**(2), 169-182 (2012)

Koroishi, E.H., Cavalini Jr, A.A., Lima, A.M., Steffen Jr, V.: Stochastic modeling of flexible rotors, J. Braz. Soc. Mech. Sci. **34**, 574-583 (2012)

Kang, C.H., Hsu, W.C., Lee, E.K., Shiau, T.N.: Dynamic analysis of gear-rotor system with viscoelastic supports under residual shaft bow effect. Mech. Mach. Theory **46**(3), 264-275 (2011)

Lu, K., Jin, Y., Chen, Y., Yang, Y., Hou, L., Zhang, Z., Li, Z., Fu, C.: Review for order reduction based on proper orthogonal decomposition and outlooks of applications in mechanical systems. Mech. Syst. Signal Process **123**, 264-297 (2019)

Lu, K., Lian, Z., Gu, F., Liu, H.: Model-based chatter stability prediction and detection for the turning of a flexible workpiece. Mech. Syst. Signal Process **100**, 814-826 (2018)

Li, B., Ma, H., Yu, X., Zeng, J., Guo, X., Wen, B.: Nonlinear vibration and dynamic stability analysis of rotor-blade system with nonlinear supports. Arch. Appl. Mech. **89**(7), 1375-1402 (2019)

Li, Z., Jiang, J., Tian, Z.: Stochastic dynamics of a nonlinear misaligned rotor system subject to random fluid-induced forces. J. Comput. Nonlin. Dyn. **12**(1), 011004 (2017)

Li, Z., Jiang, J., Tian, Z.: Non-linear vibration of an angular-misaligned rotor system with uncertain parameters. J. Vib. Control **22**(1), 129-144 (2016)

Li, J., Hong, J., Ma, Y., Zhang, D.: Modelling of misaligned rotor systems in aero-engines, in: ASME Turbo Expo 2012: International Mechanical Engineering Congress and Exposition, American Society of Mechanical Engineers, 535-543 (2012)

Liu, J., Sun, X., Meng, X., Li, K., Zeng, G., Wang, X.: A novel shape function approach of dynamic load identification for the structures with interval uncertainty. Int. J. Mech. Mater. Des. **12**(3), 375-386 (2016)

Lees, A.: Misalignment in rigidly coupled rotors. J. Sound Vib. **305**(1), 261-271 (2007)

Ma, H., Zeng, J., Feng, R., Pang, X., Wang, Q., Wen, B.: Review on dynamics of cracked gear systems. Eng. Fail. Anal. **55**, 224-245 (2015a)

Ma, H., Wang, X., Niu, H., Wen, B.: Oil-film instability simulation in an overhung rotor system with flexible coupling misalignment. Arch. Appl. Mech. **85**(7), 893-907 (2015b)

Nayfeh, A.H., Mook, D.T.: Nonlinear oscillations. John Wiley & Sons, 2008.

Patel, T.H., Darpe, A.K.: Vibration response of misaligned rotors. J. Sound Vib. **325**(3), 609-628 (2009)

Qi, W., Qiu, Z.: A collocation interval analysis method for interval structural parameters and stochastic excitation. Sci. China Phys. Mech. **55**(1), 66-77 (2012)

Qiu, Z., Wang, X.: Comparison of dynamic response of structures with uncertain-but-bounded parameters using non-probabilistic interval analysis method and probabilistic approach. Int. J. Solids Struct. **40**(20), 5423-5439 (2003)

Redmond, I.: Study of a misaligned flexibly coupled shaft system having nonlinear bearings and cyclic coupling stiffness-Theoretical model and analysis. J. Sound Vib. **329**(6), 700-720 (2010)

Roy, P.A., Meguid, S.A.: Nonlinear transient dynamic response of a blade subject to a pulsating load in a decaying centrifugal force field. Int. J. Mech. Mater. Des. **14**(4), 709-728 (2018)

Ritto, T.G., Lopez, R.H., Sampaio, R., Cursi, J.E.S.D.: Robust optimization of a flexible rotor-bearing system using the Campbell diagram. Eng. Optimiz. **43**(1), 77-96 (2011)

Soize, C.: Maximum entropy approach for modeling random uncertainties in transient elastodynamics. J. Acoust. Soc. Am. **109**(5), 1979-1996 (2001)

Sinou, J.-J., Nechak, L., Besset, S.: Kriging metamodeling in rotordynamics: Application for predicting critical speeds and vibrations of a flexible rotor. Complexity. Article ID 1264619 (2018)

Sinou, J.-J., Faverjon, B.: The vibration signature of chordal cracks in a rotor system including uncertainties. J. Sound Vib. **331**(1), 138-154 (2012)

Sinha, J.K., Lees, A., Friswell, M.I.: Estimating unbalance and misalignment of a flexible rotating machine from a single run-down. J. Sound Vib. **272**(3-5), 967-989 (2004)

Srinivas, R.Siva, Tiwari, R., Kannababu, Ch.: Model based analysis and identification of multiple fault parameters in coupled rotor systems with offset discs in the presence of angular misalignment and integrated with an active magnetic bearing. J. Sound Vib. **450**,109-140 (2019)

Tai, X., Ma, H., Liu, F., Liu, Y., Wen, B.: Stability and steady-state response analysis of a single rub-impact rotor system. Arch. Appl. Mech. **85**(1), 133-148 (2015)

Tuckmantel, F.W., Cavalca, K.L.: Vibration signatures of a rotor-coupling-bearing system under angular misalignment. Mech. Mach. Theory **133**, 559-583 (2019)

Wang, N., Jiang, D.: Vibration response characteristics of a dual-rotor with unbalance-misalignment coupling faults: Theoretical analysis and experimental study. Mech. Mach. Theory **125**, 207-219 (2018)

Wang, C., Ma, Y., Zhang, D., Hong, J.: Interval analysis on aero-engine rotor system with misalignment, in: ASME Turbo Expo 2015: Turbine Technical Conference and Exposition, American Society of Mechanical Engineers, V07AT30A002 (2015)

Wu, J., Luo, Z., Zheng, J., Jiang, C.: Incremental modeling of a new high-order polynomial surrogate model. Appl. Math. Model. **40**(7-8), 4681-4699 (2016)

Wu, J., Luo, Z., Zhang, N., Zhang, Y.: A new interval uncertain optimization method for structures using Chebyshev surrogate models. Comput. Struct. **146**, 185-196 (2015)

Wu, J., Zhang, Y., Chen, L., Luo, Z.: A Chebyshev interval method for nonlinear dynamic systems under uncertainty. Appl. Math. Model. **37**(6), 4578-4591 (2013)

Xu, M., Marangoni, R.: Vibration analysis of a motor-flexible coupling-rotor system subject to misalignment and unbalance, Part II: experimental validation. J. Sound Vib. **176**(5), 681-691 (1994)

Yang, Y., Wu, Q., Wang, Y., Qin, W., Lu, K.: Dynamic characteristics of cracked uncertain hollow-shaft. Mech. Syst. Signal Process **124**, 36-48 (2019)

List of Figures

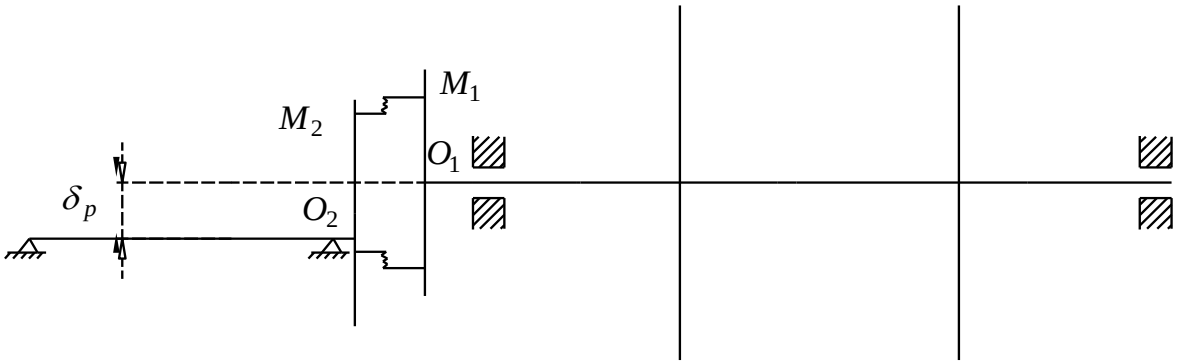

Figure 1. Schematic diagram of parallel misalignment.

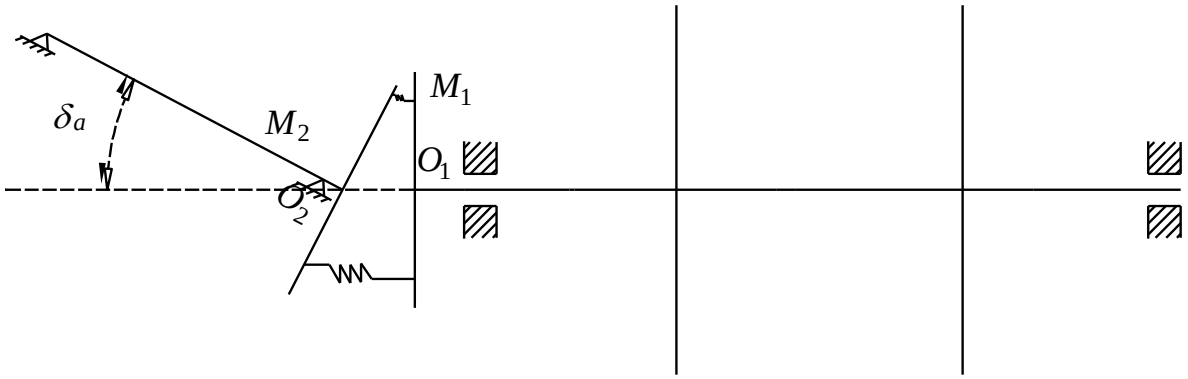

Figure 2. Schematic diagram of angular misalignment.

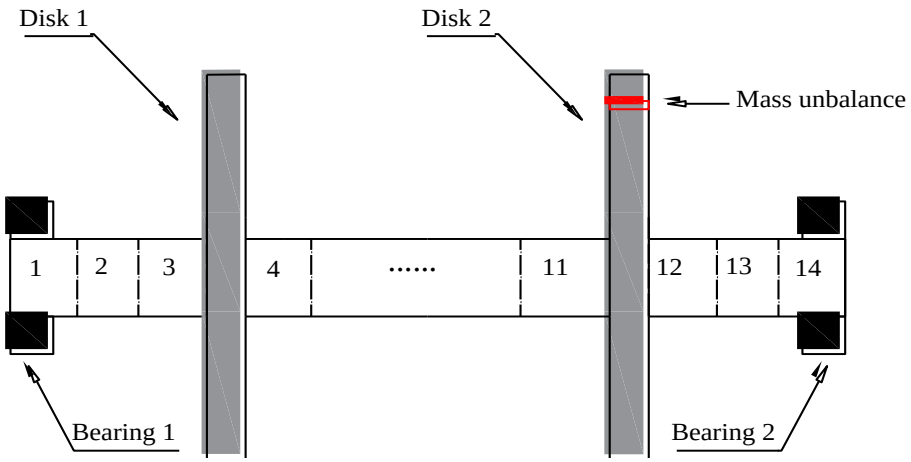

Figure 3. Academic model of the rotor system.

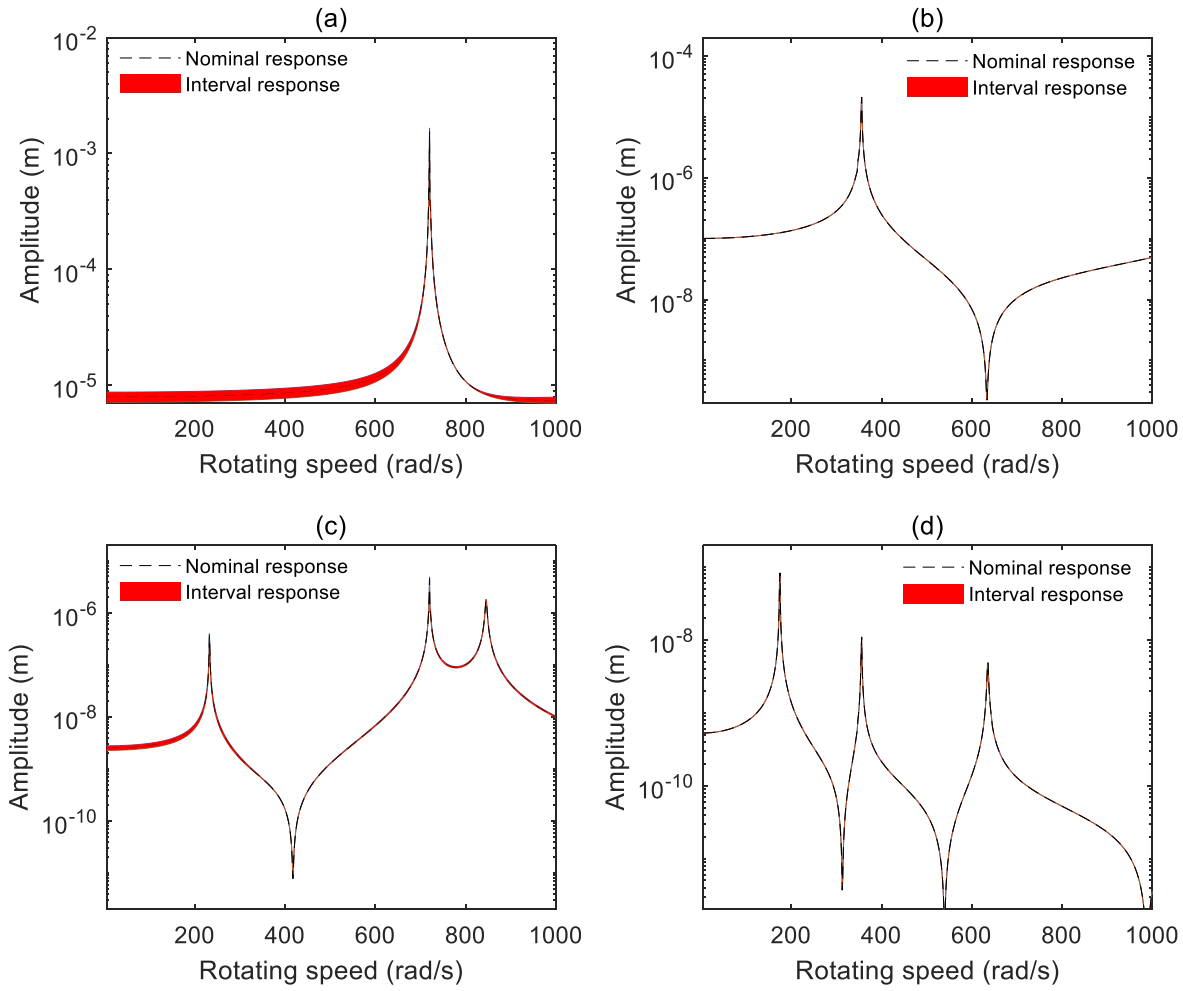

399

400 **Figure 4.** Response variability under 10% uncertainty in parallel misalignment: (a) 1× harmonic
401 component, (b) 2× harmonic component, (c) 3× harmonic component, (d) 4× harmonic
402 component.

403

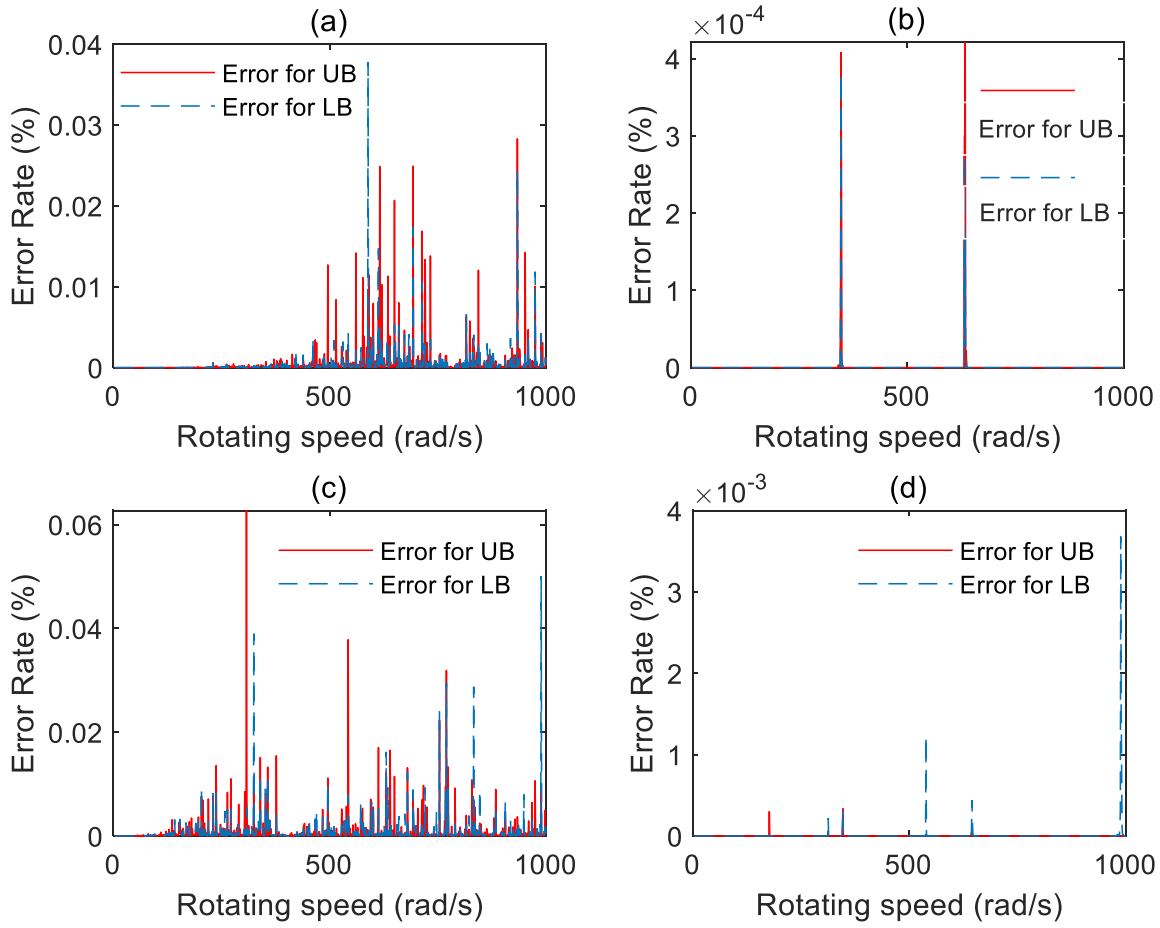

404
405 **Figure 5.** Calculation error rate: (a) 1× harmonic component, (b) 2× harmonic component, (c) 3×
406 harmonic component, (d) 4× harmonic component.

407

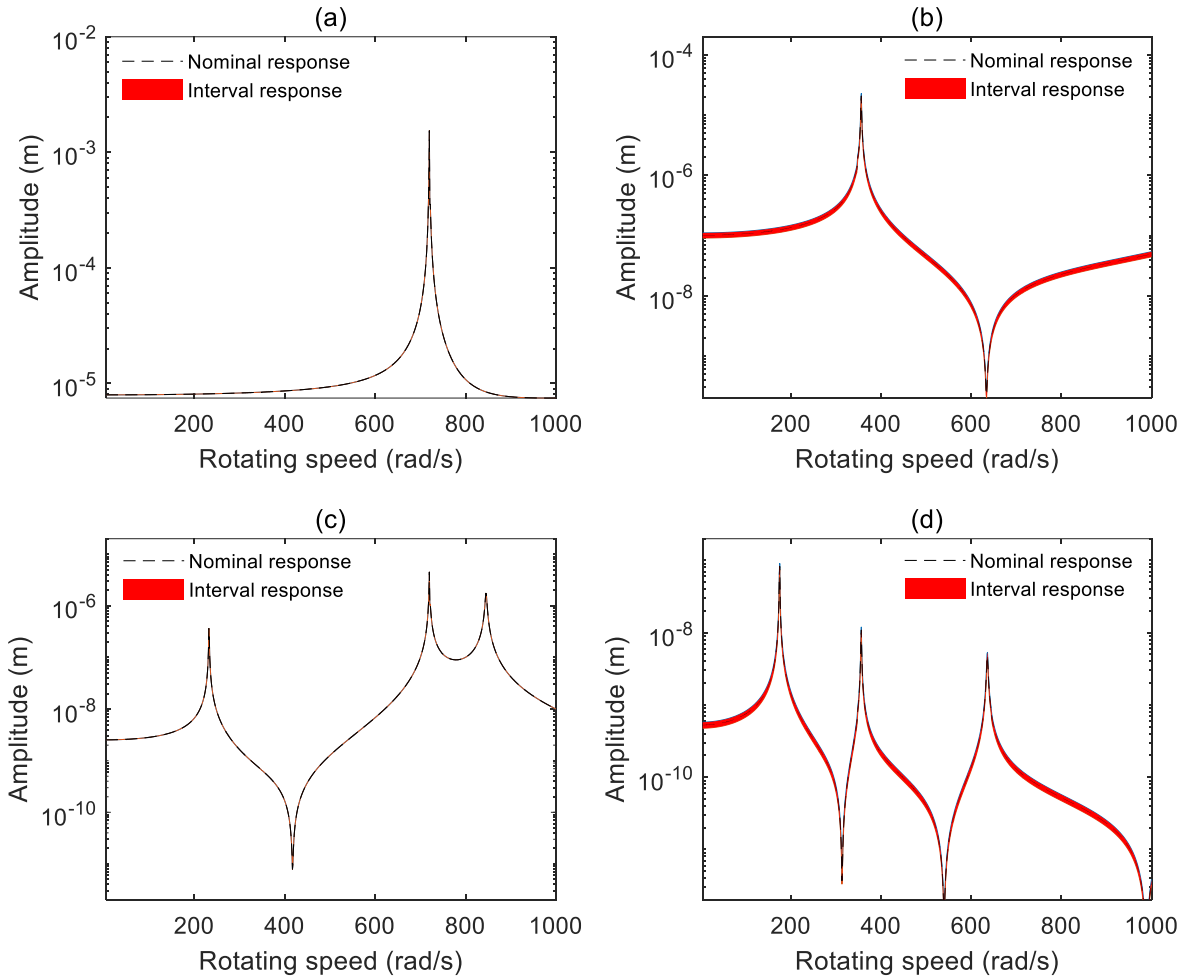

Figure 6. Response variability under 5% uncertainty in angular misalignment: (a) 1× harmonic component, (b) 2× harmonic component, (c) 3× harmonic component, (d) 4× harmonic component.

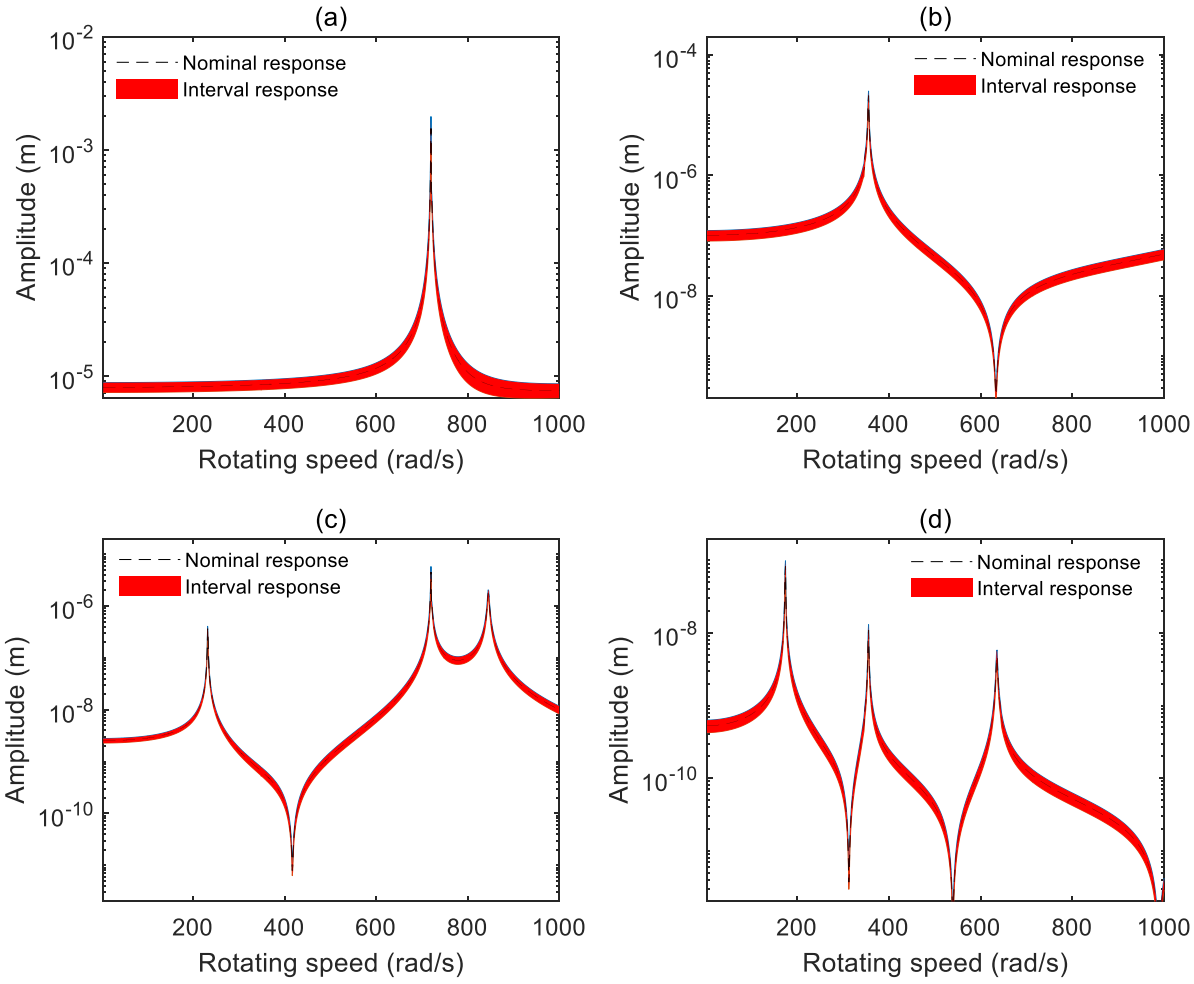

Figure 7. Response variability under multiple uncertainties: (a) 1× harmonic component, (b) 2× harmonic component, (c) 3× harmonic component, (d) 4× harmonic component.

List of Tables

Table 1. Values of parameters

Parameter	Value	Parameter	Value
Length of shaft, l	0.825 m	Young's modulus, E	2.1×10^{11} N/m^2
Axial stiffness of bolts, k_a	2×10^5 N/m	Density, ρ	7800 kg/m^3
Transverse stiffness of bolts, k_t	1×10^6 N/m	Viscous damping, C	200 N·s/m
Unbalance angle, φ	0 rad	Stiffness of bearing 1, K_1	7×10^7 N/m
Poisson's ratio, ν	0.3	Stiffness of bearing 2, K_2	7×10^7 N/m
Disk mass, m_d	0.5 kg	Mass unbalance, $m_e d$	5×10^{-5} kg·m
Radius of the disks, R_0	0.22 m	Additional stiffness, $k^{'}$	1×10^6 N/m